Free Vibration Analysis of Plate Structures Using Finite Element-Transfer Stiffness Coefficient Method

Myung-Soo Choi*

Department of Control & Mechanical Engineering, Division of Mechanical Engineering, Pukyong National University, San 100, Yongdang-Dong, Nam-Gu, Busan 608-739, Korea

In order to execute efficiently the free vibration analysis of 2-dimensional structures like plate structures, the author developed the finite element-transfer stiffness coefficient method. This method is based on the combination of the modeling techniques in the FEM and the transfer technique of the stiffness coefficient in the transfer stiffness coefficient method. Numerical results of the simply supported and the elastic supported rectangular plates showed that the present method can be successfully applied to the free vibration analysis of plate structures on a personal computer. We confirmed that, in the case of analyzing the free vibration of rectangular plate structures, the present method is superior to the FEM from the viewpoint of computation time and storage.

Key Words : Finite Element-Transfer Stiffness Coefficient Method, Finite Element Method, Free Vibration, Plate, Computation Time, Natural Frequency, Mode Shape

1. Introduction

Various numerical methods have been developed and used in static and dynamic analyses of structures. Because it is generally difficult to obtain an accurate analytical solution for structures with complicated shapes, various loads, and different material properties. Therefore, we need to rely on approximate numerical methods for obtaining acceptable solutions of static and dynamic problems.

The finite element method (FEM) is the most widely used and powerful numerical method. However, the FEM is not always the best method because it takes much computer storage and computation time in the case of solving dynamic problems accurately (Sehmi 1989). In order to develop efficient method for dynamic analysis, many researchers have studied various methods such as the transfer matrix method (TMM) (Pestel and Leckie 1963; Lee et al., 1996), the dynamic substructure method (Cheung and Leung 1991), the spectral element method (SEM) (Doyle 1997; Lee and Lee 1998), the model reduction technique (Geradin and Chen 1995), and the transfer stiffness coefficient method (TSCM) (Kondou et al., 1996; Moon and Choi 1999, 2000).

Cheung (1976) presented the finite strip method (FSM) which combines the use of Fourier expansions and one-dimensional finite elements. The FSM is an efficient analysis method for structures with regular geometry and simple boundary conditions. However, it is difficult to apply for structures with complicated shapes and different material properties.

In order to reduce structural matrix size of the FEM without loss of accuracy, the combined use of the finite element and transfer matrix was first suggested by Dokanish (1972) for the free vibration analysis of plates. This method, the finite element-transfer matrix method (FE-TMM), was

* **E-mail** : vibsound@hanmail.net
TEL : +82-51-620-1577; **FAX** : +82-51-620-1574
Department of Control & Mechanical Engineering, Division of Mechanical Engineering, Pukyong National University, San 100, Yongdang-Dong, Nam-Gu, Busan 608-739, Korea. (Manuscript **Received** August 5, 2002; **Revised** March 20, 2003)

refined by several researchers for application and improvement (Liu and Huang 1992; Ohga et al., 1993; Yuhua 1995). However, numerical instabilities occur in the TMM when it is used for calculating higher natural frequencies or responses for a flexible beam on a stiff foundation because of the propagation of round-off error in the transfer matrix. It results in undesirable and inaccurate results in the analysis of structures. Therefore, the FE-TMM contains these disadvantages of the TMM too.

Lee (2000) introduced the spectral transfer matrix method (STMM) for analyzing periodic structures efficiently. The STMM has the good features of the SEM and the TMM. However, in the case of analyzing long structures, it is difficult to apply the STMM because of the above-mentioned disadvantages of the TMM. The Riccati transfer matrix method (Horner and Pilkey 1978) was suggested as a mean of limiting the propagation of round-off errors in the TMM. Xue (1997) proposed the combined finite element-Riccati transfer matrix method and applied it to the dynamic analysis of structures.

Kondou et al. (1996) proposed the TSCM based on the transfer of the stiffness coefficient matrix related to the force and displacement vectors at each node of a beam structure, but it is limited to lumped-mass modeling. It is unable to use consistent-mass modeling. Moon and Choi (1999, 2000) refined the TSCM for application and improvement and confirmed that the technique using the transfer of stiffness coefficient is more effective than the FEM in solving accurately dynamic problems on a personal computer. However, so far the application of the TSCM has been confined to beam-like one-dimensional structures, so that we could not use the TSCM for analyzing 2-dimensional structures such as plate structures.

The purpose of this study is to extend the application of the TSCM to the plate structure. In order to execute efficiently the dynamic analysis of plate structures, the author developed the finite element-transfer stiffness coefficient method (FE-TSCM) based on the combination of modeling techniques in the FEM and the transfer technique of the stiffness coefficient in the TSCM. The merit of the FE-TSCM is to take the advantages of both methods, that is, the convenience of the modeling in the FEM and the computational efficiency of the TSCM.

In this paper, the free vibration analysis algorithm of plates is formulated by the FE-TSCM. In order to illustrate the efficiency of the FE-TSCM, two rectangular plate structures with various mesh patterns are chosen as numerical examples, and their results obtained by the FE-TSCM are compared with the FEM and the analytical solutions.

2. Theory

In order to describe clearly the concept of the FE-TSCM, a flat plate structure consisting of a rectangular plate and elastic support springs is considered as an analytical model.

2.1 Modeling

A rectangular plate is divided into m strips, as shown in Fig. 1. Sections dividing strips are called nodal lines, which are designated as nodal line 0, nodal line 1, ···, nodal line m consecutively from the left edge to the right edge of the plate. In the FE-TSCM, the boundary conditions of the plate are considered as elastic support springs. For example, in the case of the fixed condition, it is replaced by corresponding spring constant of infinite value, and in the case of the free condition, by a spring constant of 0. Intermediate rigid conditions of the structure are easily considered as the corresponding support spring constants with infinite value, too.

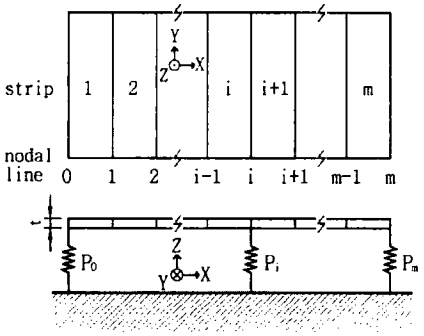

Fig. 1 Analytical model

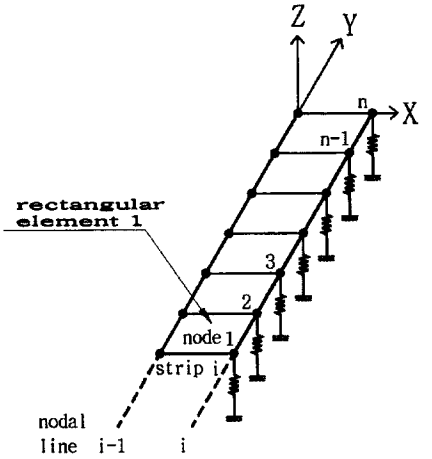

Fig. 2 Elastic support springs and strip i subdivided rectangular elements

Strip i represents the ith strip of the plate, which is between nodal line i-1 and nodal line i. Each strip is subdivided into rectangular elements and $2n$ nodes, as shown in Fig. 2. Where n nodes are on the nodal line i-1, and n nodes are on the nodal line i.

2.2 Dynamic stiffness matrix for a strip

The mass matrix $\widetilde{\mathbf{M}}_i$ and the stiffness matrix $\widetilde{\mathbf{K}}_i$ for strip i can be obtained by the assemblage of the mass matrix $\mathbf{M}$ and the stiffness matrix $\mathbf{K}$ for each rectangular element, respectively (Petyt 1990). The detailed expression of $\mathbf{M}$ and $\mathbf{K}$ are listed in the appendix.

In the case of free vibration, the equilibrium equation for strip i is given by

$$(\widetilde{\mathbf{K}}_i-\omega^2\widetilde{\mathbf{M}}_i)\,\widetilde{\mathbf{U}}_i=\widetilde{\mathbf{F}}_i \tag{1}$$

where ω is the natural frequency of the plate, $\widetilde{\mathbf{U}}_i$ and $\widetilde{\mathbf{F}}_i$ the column vectors containing displacements and forces of all nodes on the strip i. Therefore, $\widetilde{\mathbf{U}}_i$ and $\widetilde{\mathbf{F}}_i$ are composed of the displacement vector $\tilde{\mathbf{u}}$ and the force vector $\tilde{\mathbf{f}}$ of each node on strip i are as follows:

$$\begin{aligned}
&\widetilde{\mathbf{U}}_i={}^{\mathrm{T}}\{\,\widetilde{\mathbf{U}}_i^{\mathrm{L}},\ \widetilde{\mathbf{U}}_i^{\mathrm{R}}\,\},\\
&\widetilde{\mathbf{U}}_i^{\mathrm{L}}={}^{\mathrm{T}}\{\,\tilde{\mathbf{u}}_1,\ \tilde{\mathbf{u}}_2,\ \cdots,\ \tilde{\mathbf{u}}_n\,\}_i^{\mathrm{L}},\\
&\widetilde{\mathbf{U}}_i^{\mathrm{R}}={}^{\mathrm{T}}\{\,\tilde{\mathbf{u}}_1,\ \tilde{\mathbf{u}}_2,\ \cdots,\ \tilde{\mathbf{u}}_n\,\}_i^{\mathrm{R}},\\
&\widetilde{\mathbf{F}}_i={}^{\mathrm{T}}\{\,\widetilde{\mathbf{F}}_i^{\mathrm{L}},\ \widetilde{\mathbf{F}}_i^{\mathrm{R}}\,\},\\
&\widetilde{\mathbf{F}}_i^{\mathrm{L}}={}^{\mathrm{T}}\{\,\tilde{\mathbf{f}}_1,\ \tilde{\mathbf{f}}_2,\ \cdots,\ \tilde{\mathbf{f}}_n\,\}_i^{\mathrm{L}},\\
&\widetilde{\mathbf{F}}_i^{\mathrm{R}}={}^{\mathrm{T}}\{\,\tilde{\mathbf{f}}_1,\ \tilde{\mathbf{f}}_2,\ \cdots,\ \tilde{\mathbf{f}}_n\,\}_i^{\mathrm{R}}
\end{aligned} \tag{2}$$

where superscripts "L", "R" and subscript "i" represent the quantities about the left- and right-hand nodes of strip i, and superscript "T" denotes the transpose of a vector.

Equation (1) can be written as

$$\widetilde{\mathbf{S}}_i\widetilde{\mathbf{U}}_i=\widetilde{\mathbf{F}}_i \tag{3}$$

where the dynamic stiffness matrix $\widetilde{\mathbf{S}}_i$ for the strip i becomes

$$\widetilde{\mathbf{S}}_i=\widetilde{\mathbf{K}}_i-\omega^2\widetilde{\mathbf{M}}_i \tag{4}$$

The matrix $\widetilde{\mathbf{S}}_i$ can be partitioned into four square matrices $\widetilde{\mathbf{A}}_i$, $\widetilde{\mathbf{B}}_i$, $\widetilde{\mathbf{C}}_i$, $\widetilde{\mathbf{D}}_i$. Then Eq. (3) rewritten as

$$\begin{Bmatrix}\widetilde{\mathbf{F}}_i^{\mathrm{L}}\\ \widetilde{\mathbf{F}}_i^{\mathrm{R}}\end{Bmatrix}=\begin{bmatrix}\widetilde{\mathbf{A}}_i & \widetilde{\mathbf{B}}_i\\ \widetilde{\mathbf{C}}_i & \widetilde{\mathbf{D}}_i\end{bmatrix}\begin{Bmatrix}\widetilde{\mathbf{U}}_i^{\mathrm{L}}\\ \widetilde{\mathbf{U}}_i^{\mathrm{R}}\end{Bmatrix} \tag{5}$$

which is the relationship between the force and displacement vectors at the left- and right-hand nodes of strip i.

2.3 Transfer of stiffness coefficient matrix

In order to describe easily the transfer process of stiffness coefficients, a nodal line is divided into the left- and right- hand-sides of the nodal line. The right-hand section of strip i becomes the left-hand-side of nodal line i, and the left-hand section of strip $i+1$ becomes the right-hand-side of nodal line i. Therefore, Eq. (5) can be changed into

$$\begin{Bmatrix}\mathbf{F}_{i-1}\\ \bar{\mathbf{F}}_i\end{Bmatrix}=\begin{bmatrix}\mathbf{A}_i & \mathbf{B}_i\\ \mathbf{C}_i & \mathbf{D}_i\end{bmatrix}\begin{Bmatrix}\mathbf{U}_{i-1}\\ \bar{\mathbf{U}}_i\end{Bmatrix} \tag{6}$$

where

$$\begin{aligned}
&\mathbf{F}_{i-1}=-\widetilde{\mathbf{F}}_i^{\mathrm{L}},\ \bar{\mathbf{F}}_i=\widetilde{\mathbf{F}}_i^{\mathrm{R}},\ \mathbf{U}_{i-1}=\widetilde{\mathbf{U}}_i^{\mathrm{L}},\ \bar{\mathbf{U}}_i=\widetilde{\mathbf{U}}_i^{\mathrm{R}}\\
&\mathbf{A}_i=-\widetilde{\mathbf{A}}_i,\ \mathbf{B}_i=-\widetilde{\mathbf{B}}_i,\ \mathbf{C}_i=\widetilde{\mathbf{C}}_i,\ \mathbf{D}_i=\widetilde{\mathbf{D}}_i
\end{aligned} \tag{7}$$

in which $\bar{\mathbf{F}}_i$ and $\bar{\mathbf{U}}_i$ are the force and displacement vectors at the left-hand-side of nodal line i, and $\mathbf{F}_{i-1}$ and $\mathbf{U}_{i-1}$ are the force and displacement vectors at the right-hand-side of nodal line i-1, respectively. We indicate quantities of the left-hand-side of a nodal line with the head mark "—" on symbols, and the right-hand-side without the head mark. The subscript "i" of $\mathbf{F}$ and $\mathbf{U}$ means the quantity corresponding to nodal line i.

In the present method, four sub-matrices $\mathbf{A}_i$, $\mathbf{B}_i$, $\mathbf{C}_i$ and $\mathbf{D}_i$ are very easily obtained from Eq.

(7). However, in the case of the FE-TMM (Dokainish 1972), the procedure obtaining the transfer matrix from a strip modeled by the FEM is more complicated than the FE-TSCM.

We define the relationship between the force and displacement vectors at the left- and right-hand-side of nodal line i as follows:

$$\bar{\mathbf{F}}_i=\bar{\mathbf{S}}_i\bar{\mathbf{U}}_i \quad (i=1, 2, \cdots, m) \tag{8}$$

and

$$\mathbf{F}_i=\mathbf{S}_i\mathbf{U}_i \quad (i=0, 1, \cdots, m) \tag{9}$$

and we call the matrices $\bar{\mathbf{S}}_i$ and $\mathbf{S}_i$ as the stiffness coefficient matrices at the left- and right-hand-side of the nodal line i, respectively.

From Eqs. (6) and (9), the force vector $\mathbf{F}_{i-1}$ is given by

$$\mathbf{F}_{i-1}=\mathbf{A}_i\mathbf{U}_{i-1}+\mathbf{B}_i\bar{\mathbf{U}}_i=\mathbf{S}_{i-1}\mathbf{U}_{i-1} \tag{10}$$

We can derive the relationship between the displacement vectors, $\mathbf{U}_{i-1}$ and $\bar{\mathbf{U}}_i$, from Eq. (10) as follows:

$$\mathbf{U}_{i-1}=(\mathbf{S}_{i-1}-\mathbf{A}_i)^{-1}\mathbf{B}_i\bar{\mathbf{U}}_i \tag{11}$$

From Eqs. (6) and (8), the force vector $\bar{\mathbf{F}}_i$ is given by

$$\bar{\mathbf{F}}_i=\mathbf{C}_i\mathbf{U}_{i-1}+\mathbf{D}_i\bar{\mathbf{U}}_i=\bar{\mathbf{S}}_i\bar{\mathbf{U}}_i \tag{12}$$

and substituting Eq. (11) into Eq. (12), we get

$$\{\mathbf{C}_i(\mathbf{S}_{i-1}-\mathbf{A}_i)^{-1}\mathbf{B}_i+\mathbf{D}_i\}\bar{\mathbf{U}}_i=\bar{\mathbf{S}}_i\bar{\mathbf{U}}_i \tag{13}$$

Therefore, the above equation can be written as

$$\bar{\mathbf{S}}_i=\mathbf{C}_i\mathbf{V}_i+\mathbf{D}_i \quad (i=1, 2, \cdots, m) \tag{14}$$

where

$$\mathbf{V}_i=\mathbf{G}_i^{-1}\mathbf{B}_i,\ \mathbf{G}_i=\mathbf{S}_{i-1}-\mathbf{A}_i \tag{15}$$

We call Eq. (14) as the field transfer equation of stiffness coefficient matrix, which can derive the stiffness coefficient matrix $\bar{\mathbf{S}}_i$ at the left-hand-side of nodal line i from the stiffness coefficient matrix $\mathbf{S}_{i-1}$ at the right-hand-side of nodal line i-1.

If there are elastic support springs at nodal line i, as shown in Fig. 2, the equilibrium equation of force vectors and the continuous condition of displacement vectors at the nodal line i can be written as

$$\mathbf{F}_i=\bar{\mathbf{F}}_i+\mathbf{P}_i\mathbf{U}_i,\ \mathbf{U}_i=\bar{\mathbf{U}}_i \tag{16}$$

Here, the point stiffness matrix $\mathbf{P}_i$ is a diagonal matrix and consists of linear and rotational spring constants at the nodal line i as follows:

$$\mathbf{P}_i=diag(k_{Z1}, K_{X1}, K_{Y1}, k_{Z2}, K_{X2}, K_{Y2}, \cdots, k_{Zn}, K_{Xn}, K_{Yn})_i \tag{17}$$

where k_Z is the linear spring constant in the Z-direction, K_X and K_Y are the rotational spring constants in the X- and Y-directions. In the FE-TSCM, the boundary conditions of structures are modeled as the elastic support springs of the nodal line. For example, in the case of fixed condition at the left-hand edge of the plate, we consider the point stiffness matrix $\mathbf{P}_0$ of Eq. (17) as $diag(\infty, \infty, \infty, \cdots, \infty)$, in the case of free condition as $diag(0, 0, 0, \cdots, 0)$, and in the case of simply supported condition as $diag(\infty, \infty, 0, \infty, \infty, 0, \cdots)$.

If we take the stiffness coefficient matrix $\bar{\mathbf{S}}_i$ at the left-hand-side of nodal line i, we can derive the stiffness coefficient matrix $\mathbf{S}_i$ at the right-hand-side of nodal line i. By substituting Eqs. (8) and (9) in Eq. (16), the stiffness coefficient matrix $\mathbf{S}_i$ at the right-hand-side of nodal line i becoms:

$$\mathbf{S}_i=\bar{\mathbf{S}}_i+\mathbf{P}_i \quad (i=1, 2, \cdots, m) \tag{18}$$

which is called as the point transfer equation of stiffness coefficient matrix.

Therefore, if we take the stiffness coefficient matrix $\mathbf{S}_{i-1}$ at the right-hand-side of nodal line i-1, we can obtain the matrix $\mathbf{S}_i$ at the right-hand-side of nodal line i from Eqs. (14) and (18):

$$\mathbf{S}_i=\mathbf{C}_i\mathbf{V}_i+\mathbf{D}_i+\mathbf{P}_i \quad (i=1, 2, \cdots, m) \tag{19}$$

Because the boundary condition at the left-hand edge of the plate was modeled by the point stiffness matrix $\mathbf{P}_0$ at nodal line 0, the left-hand side of nodal line 0 can be considered analytically as being free ($\bar{\mathbf{F}}_0=\mathbf{0}$). Therefore, force vector $\mathbf{F}_0$ becomes $\mathbf{F}_0=\mathbf{P}_0\mathbf{U}_0=\mathbf{S}_0\mathbf{U}_0$ from Eqs. (9) and (16), and we can find out:

$$\mathbf{S}_0=\mathbf{P}_0 \tag{20}$$

After finding out the matrix $\mathbf{S}_0$ from Eq. (20), we can apply the Eq. (19) successively and obtain finally the stiffness coefficient matrix $\mathbf{S}_m$ at the right-hand-side of nodal line m.

2.4 Frequency equation

Because the boundary condition at the right-hand edge of the plate was modeled by the point stiffness matrix $\mathbf{P}_m$ at nodal line m, the right-hand-side of nodal line m can be considered analytically as being free, that is, $\mathbf{F}_m=\mathbf{0}$ and $\mathbf{U}_m \neq \mathbf{0}$. By substituting $\mathbf{F}_m=\mathbf{0}$ in Eq. (9), the following equation can be obtained

$$\mathbf{S}_m\mathbf{U}_m=\mathbf{0} \tag{21}$$

and it is essential that the determinant of the matrix $\mathbf{S}_m$ is zero.

$$\det \mathbf{S}_m(\omega)=0 \tag{22}$$

In the transfer process of the stiffness coefficient matrix $\mathbf{S}_i$, we have to calculate the inverse matrix of the matrix $\mathbf{G}_i$. When the determinant of matrix $\mathbf{G}_i$ is zero, elements of the matrix $\mathbf{S}_i$ become usually asymmetric poles that change their sign before and after the poles of elements. Therefore, elements of the matrix $\mathbf{S}_m$ in Eq. (22) may contain asymmetric poles. If we use root-solving techniques (Gerald and Wheatley 1989), such as the bisection method and the linear interpolation method, for obtaining the true roots (natural frequencies) from Eq. (22), we may misconceive false roots which are undesirable and inaccurate as natural frequencies.

However, these false roots can be eliminated by applying the following technique. This technique introduces the sign function to eliminate asymmetric poles. Asymmetric poles can be transformed into symmetric poles by multiplying the sign function of the determinant of matrix $\mathbf{S}_m$ by the sign functions of the determinant of matrix $\mathbf{G}_i$ ($i=1, 2, 3, \cdots, m$).

$$Z=\prod_{i=1}^{m}\{\operatorname{sgn}(\det\mathbf{G}_i)\}\times\operatorname{sgn}(\det\mathbf{S}_m) \tag{23}$$

Therefore, we can obtain only true roots, that is, natural frequencies, by applying the bisection method to Eq. (23). In this case, the bisection method needs only the sign of the function value.

When we obtain the natural frequencies of the plate by the FEM, the size of the matrix is equal to the total number of degrees of freedom for the plate. However, in the case of using the FE-TSCM, it is greatly reduced to the number of degrees of freedom for the last nodal line, that is, the size of matrix $\mathbf{S}_m$. Therefore, it is found that the FE-TSCM is more efficient than the FEM from the viewpoint of computer storage.

2.5 Characteristic modes

Substituting Eq. (15) in Eq. (11), the relationship of displacement vectors at both nodal lines of strip i is given as follows:

$$\mathbf{U}_{i-1}=\mathbf{V}_i\bar{\mathbf{U}}_i \quad (i=m, m-1, \cdots, 1) \tag{24}$$

After obtaining natural frequencies of the plate, the characteristic modes of the plate are computed from the right-hand edge to the left-hand edge, successively. The displacement vector of the nodal line m is calculated as follows: after one displacement element in the displacement vector of the nodal line m has a reference value, the other displacement elements in the displacement vector of the nodal line m are calculated form Eq. (21). Displacement vectors at the other nodal lines can be obtained by using recursively $\mathbf{U}_i=\bar{\mathbf{U}}_i$ in Eq. (16) and Eq. (24).

3. Numerical Examples

In order to illustrate the computation efficiency of the FE-TSCM, we made computer programs by the FE-TSCM and the FEM for analyzing the flexural free vibration of rectangular plate structures. The results obtained by FE-TSCM were compared with those obtained by the FEM and the analytical solution on a personal computer (CPU : Pentium II, Memory : 64 M Byte).

In the numerical examples, strips were made up of several thin rectangular elements with four nodes and three degrees of freedom at each node. The displacement vector at each node consisted of a displacement normal to the plane of the plate, w, and two rotations $\theta_X=\dfrac{\partial w}{\partial x}$ and $\theta_Y=\dfrac{\partial w}{\partial y}$. The displacement vector of a nodal line with n nodes is as follows:

$$\mathbf{U}_i={}^{\mathrm{T}}\{w_1, \theta_{X1}, \theta_{Y1}, w_2, \theta_{X2}, \theta_{Y2}, \cdots, w_n, \theta_{Xn}, \theta_{Yn}\}_i$$

3.1 Example 1: a rectangular plate with 4 simply supported edges

Example 1 is a rectangular plate structure which is simply supported on all four edges. The physical parameters of example 1 are as follows : length 1 m, width 0.4 m, thickness 5 mm, Young's modulus 206 GPa, density 7860 kg/m^3, and Poisson's ratio 0.3. In the numerical calculation, the rectangular plate is divided into 10×4, 15×6, 20×8, 25×10, 40×16, and 80×32 mesh patterns.

Figure 3 shows the rectangular plate divided into a 10×4 mesh pattern with 10 strips, 40 rectangular elements, 55 nodes, and 165 degrees of freedom.

Table 1 shows first twenty natural frequencies of example 1 with 10×4, 20×8, 40×16, and 80×32 mesh patterns by the FEM, the FE-TSCM, and the analytical solution (Timoshenko and Young 1974). In Table 1, (m, n) is the number of half-waves in the X- and Y-directions.

When the plate is divided into 10×4 and 20×8 mesh patterns, the natural frequencies of the plate obtained by the FE-TSCM agreed with those obtained by the FEM. When the plate is divided into 40×16 and 80×32 mesh patterns, natural frequencies of the plate could be obtained by the FE-TSCM on a personal computer. However, in 40×16 and 80×32 mesh patterns, we could not obtain natural frequencies of the plate by the FEM on the same personal computer. As the number of plate elements increases, the size of the global mass matrix and the global stiffness matrix becomes larger in the FEM. Because the algorithm of the FEM have to use the large global matrices at the same time in the case of 40×16 and 80×32 mesh patterns, it needs large computer storage. Therefore, it is difficult to calculate the

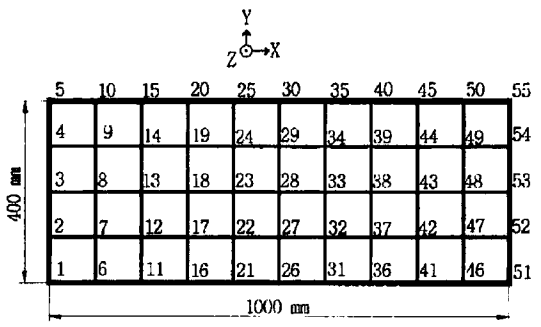

Fig. 3 A rectangular plate with 10×4 mesh pattern

Table 1 Natural frequencies for example 1 (unit : Hz)

Mode (m, n)	FEM & FE-TSCM		FE-TSCM		Analytical Solution
	10×4	20×8	40×16	80×32	
1 (1, 1)	87	88	88	88	88
2 (2, 1)	122	124	125	125	125
3 (3, 1)	179	184	185	185	186
4 (4, 1)	260	268	270	271	271
5 (1, 2)	315	316	316	316	316
6 (2, 2)	343	350	352	353	353
7 (5, 1)	365	376	379	380	380
8 (3, 2)	392	407	412	413	414
9 (4, 2)	462	487	496	498	499
10 (6, 1)	496	508	512	514	514
11 (5, 2)	555	590	603	607	608
12 (7, 1)	652	664	670	672	672
13 (1, 3)	673	696	696	696	697
14 (2, 3)	704	717	731	733	733
15 (6, 2)	725	727	735	740	742
16 (3, 3)	762	780	790	793	794
17 (8, 1)	816	845	852	854	855
18 (4, 3)	819	855	872	877	879
19 (7, 2)	838	867	891	898	900
20 (5, 3)	898	951	978	986	989

natural frequencies of the plate with large mesh pattern on the personal computer.

The results by the FEM and the FE-TSCM converged to the analytical solutions, as the number of rectangular elements increaseds.

Table 2 shows computation time used for obtaining natural frequencies of example 1 with 10×4, 15×6, 20×8, and 25×10 mesh patterns by the FEM and the FE-TSCM. It was found from Table 2 that the FEM has a little advantage in computation time for the plate with a small number of elements, but the FE-TSCM has a greater advantage for the plate with many elements.

Table 2 Computation times for example 1

(unit : sec)

Method	Mesh pattern			
	10×4	15×6	20×8	25×10
FEM	8	73	413	1444
FE-TSCM	15	40	85	166

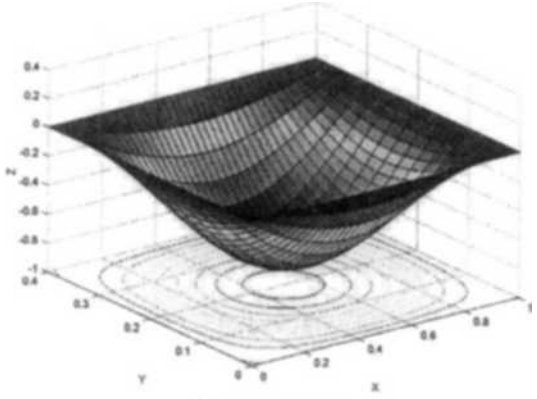

(a) First mode

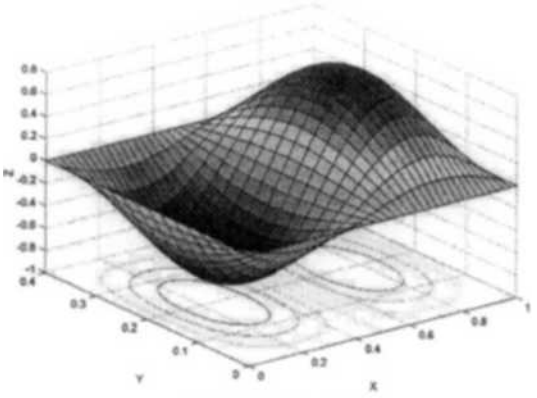

(b) Second mod

Fig. 4 Mode shapes of a simply supported plate

Figure 4 shows the first and the second mode shapes calculated by the FE-TSCM for the simply supported rectangular plate with the 40×16 mesh pattern.

3.2 Example 2 : a plate with elastic support springs at center and 4 corners

Example 2 is a rectangular plate structure with five elastic support springs(k_z=1.0E10 N/m), as shown in Fig. 5. The physical parameters of example 2 are identical with those for example 1. In the numerical calculation, the rectangular plate was divided into 10×4, 16×6, 20×8, 26×10, 40×16, and 80×32 mesh patterns.

Table 3 shows first twenty-five natural frequencies obtained by the FE-TSCM and the FEM for example 2 with 10×4, 20×8, 40×16, and 80×32 mesh patterns.

When the plate is divided into 10×4 and 20×8 mesh patterns, the natural frequencies of the plate obtained by the FE-TSCM agree with those obtained by the FEM. When the plate is divided into 40×16 and 80×32 mesh patterns, we could not obtain natural frequencies of the plate by the FEM on the same personal computer. The results by the FEM and the FE-TSCM using small mesh patterns converged to those of the FE-TSCM using large mesh patterns.

Table 4 shows computation time spert for obtaining natural frequencies of example 2 by the FEM and the FE-TSCM. As the number of rectangular elements increaseds, the FE-TSCM has much advantage in computation time too.

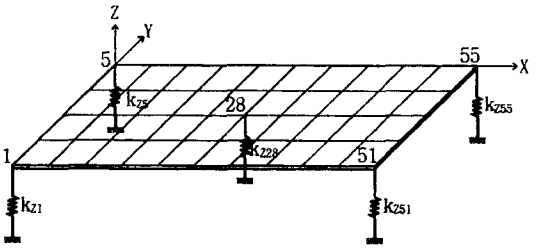

Fig. 5 A rectangular plate with five elastic support springs

Table 3 Natural frequencies for example 2
(unit : Hz)

Mode	FEM & FE-TSCM		FE-TSCM	
	10×4	20×8	40×16	80×32
1	41	41	41	41
2	45	44	44	44
3	62	62	62	62
4	92	92	92	92
5	105	104	104	104
6	114	113	113	113
7	159	158	158	158
8	177	177	177	177
9	218	217	217	217
10	241	239	238	238
11	244	245	246	246
12	272	275	275	275
13	327	324	322	322
14	376	375	375	375
15	396	391	389	389
16	415	420	422	422
17	434	438	440	441
18	451	448	446	446
19	501	503	503	504
20	513	509	508	508
21	520	523	524	524
22	582	588	591	591
23	612	625	630	631
24	653	657	661	662
25	656	667	668	667

Table 4 Computation times for example 2
(unit : sec)

Method	Mesh pattern			
	10×4	16×6	20×8	26×10
FEM	10	109	438	1783
FE-TSCM	12	33	67	135

It is found from the above Tables that we have to increase the partition number of the plate in order to obtain accurate natural frequency values, then the FE-TSCM is more effective than the FEM in computation time and computer storage.

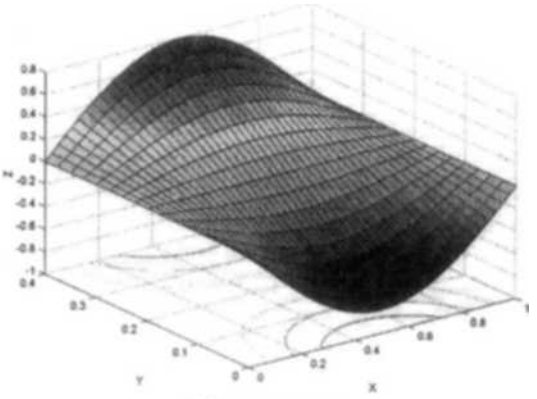

(a) First mode

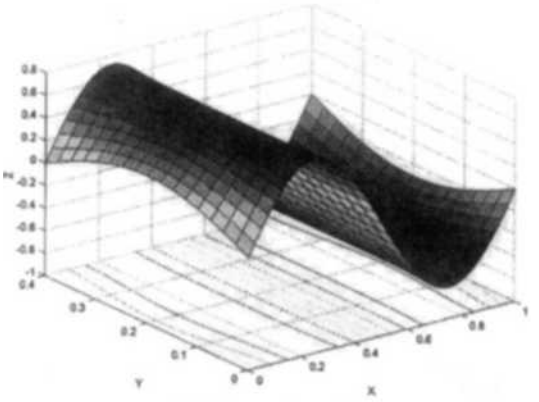

(b) Second mode

Fig. 6 Mode shapes of an elastic supported plate

Figure 6 shows the first and the second mode shapes for the elastic supported rectangular plate with a 40×16 mesh pattern by the FE-TSCM.

4. Conclusions

In order to execute efficiently the free vibration analysis of plate structures on a personal computer, the finite element-transfer stiffness coefficient method was formulated in this paper. The proposed method is based on the combination of modeling techniques in the finite element method and the transfer technique of the stiffness coefficient in the transfer stiffness coefficient method. The merit of the present method is to take the advantages of both the FEM and the TSCM, that is, the convenience of the modeling in the FEM and the computation efficiency of the TSCM.

Numerical results about the simply supported and the elastic supported rectangular plates showed that the present method can be successfully applied to the free vibration analysis of plate structures on a personal computer. We confirmed that, in the case of analyzing the free vibration of rectangular plate structures, the present method is superior to the finite element method from the viewpoint of computation time and computer storage.

Acknowledgment

This work was partially supported by the Brain Korea 21 Project in 2003.

References

Cheung, Y. K., 1976, *Finite Strip Method in Structural Analysis*, Pergamon Press, Oxford.

Cheung, Y. K. and Leung, A. Y. T., 1991, *Finite Element Methods in Dynamics*, Kluwer Academic, London.

Doyle, J. F., 1997, *Wave Propagation in Structures : Spectral Analysis Using Fast Discrete Fourier Transforms*, 2nd edition, Springer-Verlag, New York, pp. 150~197.

Dokainish, M. A., 1972, "A New Approach for Plate Vibrations : Combination of Transfer Matrix and Finite Element Technique," *Trans. of the ASME Journal of Engineering for Industry*, Vol. 94, pp. 526~530.

Geradin, M. and Chen, S. L., 1995, "An Exact Model Reduction Technique for Beam Structures : Combination of Transfer and Dynamic Stiffness Matrices," *J. of Sound and Vibration*, Vol. 185, No. 3, pp. 431~440.

Gerald, C. F. and Wheatley, P. O., 1989, *Applied Numerical Analysis*, 4th edition, Addison-Wesley, New York.

Horner, G. C. and Pilkey, W. D., 1978, "The Riccati Transfer Matrix Method," *Trans. of the ASME Journal of Mechanical Design*, Vol. 100, pp. 297~302.

Kondou, T., Ayabe, T. and Sueoka, A., 1996, "Transfer Stiffness Coefficient Method Combined with the Concept of Substructure Synthesis Method (Linear Free and Forced Vibration Analyses of a Straight-Line Beam Structure)," *Trans. of the Japan Society of Mechanical Engineering (C)*, Vol. 62, No. 596, pp. 1277~1284.

Lee, D. M., Choi M. J. and Oh T. Y., 1996, "Transfer Matrix Modelling for the 3-Dimensional Vibration Analysis of Piping System Containing Fluid Flow," *KSME Inter. J.*, Vol. 10, No. 2, pp. 180~189.

Lee, U. and Lee, J., 1998, "Vibration Analysis of the Plates Subject to Distributed Dynamic Loads by Using Spectral Element Method," *KSME Inter. J.*, Vol. 12, No. 4, pp. 565~571.

Lee, U., 2000, "Vibration Analysis of One-Dimensional Structures Using the Spectral Transfer Matrix Method," *Engineering Structures*, Vol. 22, No. 6, pp. 681~690.

Liu, W. H. and Huang, C. C., 1992, "Vibration Analysis of Folded Plates," *J. of Sound and Vibration*, Vol. 157, No. 1, pp. 123~137.

Moon, D. H. and Choi, M. S., 1999, "Vibration Analysis of Structures Having Various Connection Parts Using Transfer of Stiffness Coefficient," *Trans. of the KSME*, Vol. 23, No. 2, pp. 344~356.

Moon, D. H. and Choi, M. S., 2000, "Vibration Analysis for Frame Structures Using Transfer of Dynamic Stiffness Coefficient Method," *J. of Sound and Vibration*, Vol. 234, No. 5, pp. 725~736.

Ohga, M., Shigematsu, T. and Hara, T., 1993, "A Finite Element-Transfer Matrix Method for Dynamic Analysis of Frame Structures," *J. of Sound and Vibration*, Vol. 167 No. 3, pp. 401~411.

Pestel, E. C. and Leckie, F. A., 1963, *Matrix Methods in Elastomechanics*, McGraw-Hill, New York.

Petyt, M., 1990, *Introduction to Finite Element Vibration Analysis*, Cambridge university, New York.

Sehmi, N. S., 1989, *Large Order Structural Eigenanalysis Techniques Algorithm for Finite Element Systems*, Ellis Horwood, New York.

Timoshenko, S. and Young, D. H., 1974, *Vibration Problems in Engineering*, John Wiley & Sons, New York.

Xue, H., 1997, "A Combined Finite Element-Riccati Transfer Matrix Method in Frequency Domain for Transient Structural Response," *Computers and Structures*, Vol. 62, No. 2, pp. 215~220.

Yuhua, C., 1995, "Large Deflection Analysis of Structures by an Improved Combined Finite Element-Transfer Matrix Method," *Computers and Structures*, Vol. 55, No. 1, pp. 167~171.

Appendix

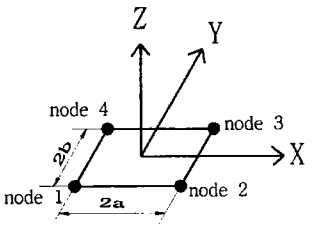

Fig. A.1 A rectangular element

The mass matrix for a rectangular element is

$$\mathbf{M}=\frac{\rho hab}{6300}\begin{bmatrix}\mathbf{M}_{11} & \mathbf{M}_{21}^{T}\\ \mathbf{M}_{21} & \mathbf{M}_{22}\end{bmatrix} \tag{A1}$$

where ρ denotes density, h is plate thickness, and

$$\mathbf{M}_{11}=\begin{bmatrix} 3454 & & & & & \\ 922b & 320b^2 & & & Sym & \\ -922a & -252ab & 320a^2 & & & \\ 1226 & 398b & -548a & 3454 & & \\ 398b & 160b^2 & -168ab & 922b & 320b^2 & \\ 548a & 168ab & -240a^2 & 922a & 252ab & 320a^2 \end{bmatrix} \tag{A2}$$

$$\mathbf{M}_{21}=\begin{bmatrix} 394 & 232b & -232a & 1226 & 548b & 398a \\ -232b & -120b^2 & 112ab & -548b & -240b^2 & -168ab \\ 232a & 112ab & -120a^2 & 398a & 168ab & 160a^2 \\ 1226 & 548b & -398a & 394 & 232b & 232a \\ -548b & -240b^2 & 168ab & -232b & -120b^2 & -112ab \\ -398a & -168ab & 160a^2 & -232a & -112ab & -120a^2 \end{bmatrix} \tag{A3}$$

$$\mathbf{M}_{22}=\begin{bmatrix} 3454 & & & & & \\ -922b & 320b^2 & & & Sym & \\ 922a & -252ab & 320a^2 & & & \\ 1226 & -398b & 548a & 3454 & & \\ -398b & 160b^2 & -168ab & -922b & 320b^2 & \\ -548a & 168ab & -240a^2 & -922a & 252ab & 320a^2 \end{bmatrix} \tag{A4}$$

The stiffness matrix for a rectangular element is

$$\mathbf{K}=\frac{Eh^3}{48(1-v^2)ab}\begin{bmatrix}\mathbf{K}_{11} & \mathbf{K}_{21}^{T}\\ \mathbf{K}_{21} & \mathbf{K}_{22}\end{bmatrix} \tag{A5}$$

where E denotes Young's modulus, v is Poisson's ratio, and

$$\mathbf{K}_{11}=\begin{bmatrix} k_1 & & & & & \\ k_2 & k_3 & & & Sym & \\ k_4 & k_5 & k_6 & & & \\ k_7 & k_8 & k_9 & k_1 & & \\ k_8 & k_{10} & 0 & k_2 & k_3 & \\ -k_9 & 0 & k_{11} & -k_4 & -k_5 & k_6 \end{bmatrix} \tag{A6}$$

$$\mathbf{K}_{21}=\begin{bmatrix} k_{12} & k_{13} & k_{14} & k_{17} & k_{18} & -k_{19} \\ -k_{13} & k_{15} & 0 & -k_{18} & k_{20} & 0 \\ -k_{14} & 0 & k_{16} & -k_{19} & 0 & k_{21} \\ k_{17} & k_{18} & k_{19} & k_{12} & k_{13} & -k_{14} \\ -k_{18} & k_{20} & 0 & -k_{13} & k_{15} & 0 \\ k_{19} & 0 & k_{21} & k_{14} & 0 & k_{16} \end{bmatrix} \tag{A7}$$

$$\mathbf{K}_{22}=\begin{bmatrix} k_1 & & & & & \\ -k_2 & k_3 & & & Sym & \\ -k_4 & k_5 & k_6 & & & \\ k_7 & -k_8 & -k_9 & k_1 & & \\ -k_8 & k_{10} & 0 & -k_2 & k_3 & \\ k_9 & 0 & k_{11} & k_4 & -k_5 & k_6 \end{bmatrix} \tag{A8}$$

where

$$k_1=4(\alpha^2+\beta^2)+\frac{2}{5}(7-2v) \tag{A9}$$

$$k_2=2b\left\{2\alpha^2+\frac{1}{5}(1+4v)\right\} \tag{A10}$$

$$k_3=4b^2\left\{\frac{4}{3}\alpha^2+\frac{4}{15}(1-v)\right\} \tag{A11}$$

$$k_4=2a\left\{-2\beta^2-\frac{1}{5}(1+4v)\right\} \tag{A12}$$

$$k_5=-4vab \tag{A13}$$

$$k_6=4a^2\left\{\frac{4}{3}\beta^2+\frac{4}{15}(1-v)\right\} \tag{A14}$$

$$k_7=-\left\{2(2\beta^2-\alpha^2)+\frac{2}{5}(7-2v)\right\} \tag{A15}$$

$$k_8=2b\left\{\alpha^2-\frac{1}{5}(1+4v)\right\} \tag{A16}$$

$$k_9=2a\left\{2\beta^2+\frac{1}{5}(1-v)\right\} \tag{A17}$$

$$k_{10}=4b^2\left\{\frac{2}{3}\alpha^2-\frac{4}{15}(1-v)\right\} \tag{A18}$$

$$k_{11}=4a^2\left\{\frac{2}{3}\beta^2-\frac{1}{15}(1-v)\right\} \tag{A19}$$

$$k_{12}=-\left\{2(\alpha^2+\beta^2)-\frac{2}{5}(7-2v)\right\} \quad \text{(A20)}$$

$$k_{13}=2b\left\{-\alpha^2+\frac{1}{5}(1-v)\right\} \quad \text{(A21)}$$

$$k_{14}=2a\left\{\beta^2-\frac{1}{5}(1-v)\right\} \quad \text{(A22)}$$

$$k_{15}=4b^2\left\{\frac{1}{3}\alpha^2+\frac{1}{15}(1-v)\right\} \quad \text{(A23)}$$

$$k_{16}=4a^2\left\{\frac{1}{3}\beta^2+\frac{1}{15}(1-v)\right\} \quad \text{(A24)}$$

$$k_{17}=2(\beta^2-2\alpha^2)-\frac{2}{5}(7-2v) \quad \text{(A25)}$$

$$k_{18}=2b\left\{-2\alpha^2-\frac{1}{5}(1-v)\right\} \quad \text{(A26)}$$

$$k_{19}=2a\left\{-\beta^2+\frac{1}{5}(1+4v)\right\} \quad \text{(A27)}$$

$$k_{20}=4b^2\left\{\frac{2}{3}\alpha^2-\frac{1}{15}(1-v)\right\} \quad \text{(A28)}$$

$$k_{21}=4a^2\left\{\frac{2}{3}\beta^2-\frac{4}{15}(1-v)\right\} \quad \text{(A29)}$$

$$\alpha=\frac{a}{b},\ \beta=\frac{b}{a} \quad \text{(A30)}$$